

## Extended X-Ray-Absorption Fine Structure of Surface Atoms on Single-Crystal Substrates: Iodine Adsorbed on Ag(111)

P. H. Citrin, P. Eisenberger, and R. C. Hewitt  
*Bell Laboratories, Murray Hill, New Jersey 07974*  
(Received 13 February 1978)

An Auger variant of the x-ray-absorption fine-structure (EXAFS) technique has been successfully applied to study the adsorption site and adsorbate-substrate bond length in a single-crystal system. The surface-EXAFS technique should have widespread applications in surface crystallographic studies.

One of the most fundamental, yet elusive, questions in surface science concerns the bond length and position of an atom adsorbed on a single-crystal surface. The interpretive difficulties associated with multiple-scattering processes in low-energy electron diffraction (LEED) are well documented,<sup>1</sup> and the need for a straightforward experimental procedure to measure these surface structural parameters is long overdue. In this Letter we report the first direct determination of an adsorbate-substrate bond length and the site of adsorption on a single-crystal surface using the technique of extended x-ray-absorption fine structure (EXAFS). The prototype  $(\sqrt{3} \times \sqrt{3})R30^\circ$  structure of I adsorbed on Ag(111) was studied here for purposes of comparison with the LEED work of Forstmann, Berndt, and Bütner<sup>2</sup> on the same system. Our new surface-EXAFS (SEXAFS) results are in very good agreement with that earlier study,<sup>2</sup> but because of the absence of multiple scattering they are significantly easier to interpret and are more accurate by over a factor of 4. Preliminary SEXAFS results from a somewhat higher coverage of I on Ag(111) have been reported previously<sup>3</sup> and are presented here for signal-noise comparison with the  $\frac{1}{3}$ -monolayer  $(\sqrt{3} \times \sqrt{3})R30^\circ$  system. General and future applications of the SEXAFS technique are also discussed.

In the SEXAFS experiment, which was performed at the Stanford Synchrotron Radiation Laboratory, the intensity of adsorbate core Auger electrons is monitored as a function of incident photon energy.<sup>4</sup> The basic principle underlying the Auger-EXAFS technique is the same as in conventional transmission-EXAFS experiments, namely the modulation with photon energy of the photoabsorption cross section by interference between outgoing and backscattered core photoelectron waves. Since each photoabsorption event ultimately results in the emission of either a characteristic x ray or an Auger electron, the intensity of either decay product must be directly

proportional to the photoabsorption cross section. In essence, the Auger-EXAFS detection scheme is the nonradiative analog of the fluorescence-EXAFS technique, which has been previously described.<sup>5</sup>

Directly measuring Auger emission from the adsorbate atoms with an energy analyzer discriminates against background emission from the substrate, and thus significantly improves the signal/background over transmission-EXAFS experiments. Nevertheless, in order to obtain sufficiently good counting statistics from so few absorbers in the synchrotron beam—about  $10^{13}$  atoms, or  $10^6$  fewer atoms than are typically analyzed from EXAFS of bulk systems—it is essential both to increase the brightness of the present-day synchrotron beam with a doubly bent focusing mirror and to perform signal averaging. After  $\sim 1$ -eV monochromatization of the 2.5-mm  $\times$  1.5-mm focused x-ray beam, the incident flux on the sample approached  $10^{11}$  photons/sec. Total data accumulation for the  $\frac{1}{3}$ -monolayer system consisted of approximately 6 h of summed 20-min scans.

The SEXAFS measurements were made at a base pressure of  $4 \times 10^{-10}$  Torr in a vacuum chamber isolated from the He atmosphere of the synchrotron beam by a 250- $\mu$ m Be window. In the same chamber, single-crystal Ag(111) was cleaned by repeated Ar-ion sputtering and annealing, and was characterized by LEED and Auger-electron spectroscopy. Iodine was adsorbed onto the room-temperature substrate at  $2 \times 10^{-8}$  Torr while its LEED pattern was continuously monitored. A detailed LEED and Auger study of the I-Ag(111) system as a function of I exposure will be reported elsewhere.<sup>6</sup> Immediately upon observation of the  $(\sqrt{3} \times \sqrt{3})R30^\circ$  pattern, admission of I was stopped, the base pressure was restored, and the I-Ag(111) system was cooled to 110°K where it remained during the course of the experiments. Surface integrity and cleanliness were inspected periodically. The crystal surface

was oriented at approximately  $20^\circ$  with respect to the direction of the synchrotron beam, i.e.,  $70^\circ$  with respect to the polarization of the beam. The 3300-eV  $L_3M_{4,5}M_{4,5}$  Auger electrons from adsorbed iodine were recorded with a commercial cylindrical mirror analyzer. The positive bias voltage on the sample and the analyzer pass energy were adjusted to optimize the signal/background. Onset of  $I(L_3M_{4,5}M_{4,5})$  Auger emission was observed at a photon energy of about 4560 eV, corresponding to the  $I(L_3)$  binding energy. The ratio of Auger electron intensity to incident photon flux was recorded as a function of photon energy, which was scanned about 300 eV above the  $I(L_3)$  "edge."

The raw SEXAFS data of the  $(\sqrt{3} \times \sqrt{3})R30^\circ$  structure is shown as curve A in Fig. 1(a). To aid in identifying the low-frequency fine structure from the high-frequency noise, we have overlaid

the transmission EXAFS data from bulk AgI (curve C, discussed below) onto the SEXAFS data. For signal/noise comparison purposes we also show the raw SEXAFS data, curve B, for an I coverage of  $\theta \sim 1-2$  monolayers on Ag(111). Because of its more complicated structure,<sup>6</sup> this higher-coverage phase will be treated in a separate work. With extensively tested analysis procedures described in detail elsewhere,<sup>7</sup> the raw data are truncated between 20 and 250 eV above the  $I(L_3)$  edge and a smooth polynomial spline background is subtracted, and after the data are converted to final-state electron wave vector,  $k$ , they are multiplied by  $k^2$ . The result is shown in Fig. 1(b). The Fourier transform of that spectrum [see Fig. 1(c)] enables the first nearest-neighbor peaks at  $R \sim 1.6-2.6$  Å to be distinguished from the noise components at higher frequencies. The peak at  $\sim 1.6$  Å is a Ramsauer-Townsend resonance which occurs generally in the back-scattering phase shift of high- $Z$  atoms. Because the intensity and position of that peak are sensitive to low-frequency background subtractions, however, we include only the main peak at  $\sim 2.6$  Å in our analysis of distance and amplitude.<sup>8</sup> A smooth window function from  $R = 1.6$  to  $3.8$  Å is used to filter out the 1.6-Å and multiple high-frequency components, and the result is retransformed back into  $k$  space to give the smooth line superposed on the raw data in Fig. 1(b). The unsystematic misfit in amplitude and phase between the raw and filtered data is almost solely due to the omission of the 1.6-Å peak,<sup>8</sup> but ultimately (see below) we are interested only in differences between the filtered I-Ag(111) and AgI data.

For our study, the filtered SEXAFS spectrum in Fig. 1(b) can be appropriately described by

$$\chi(k) = A(k) \sin[2kR + \varphi(k)],$$

where  $R$  is the I-Ag distance,  $\varphi(k)$  is the phase shift due to the potentials of the I-Ag atom pair, and  $A(k)$  is the amplitude function (normalized to the edge jump), to be discussed below. It is by now established that because  $\varphi(k)$  is chemically transferable,<sup>9</sup> it can be reliably obtained using model compounds<sup>7,9</sup> with similar pair-distribution functions<sup>10</sup> to allow determinations of  $R$  from EXAFS data of a wide variety of systems to within 0.02-Å accuracy. To analyze the I-Ag(111) system studied here, we have empirically determined the effective I-Ag phase shift from polycrystalline  $\gamma$ -AgI. The room-temperature AgI  $L_3$ -edge EXAFS data were obtained by conventional transmission detection procedures and were

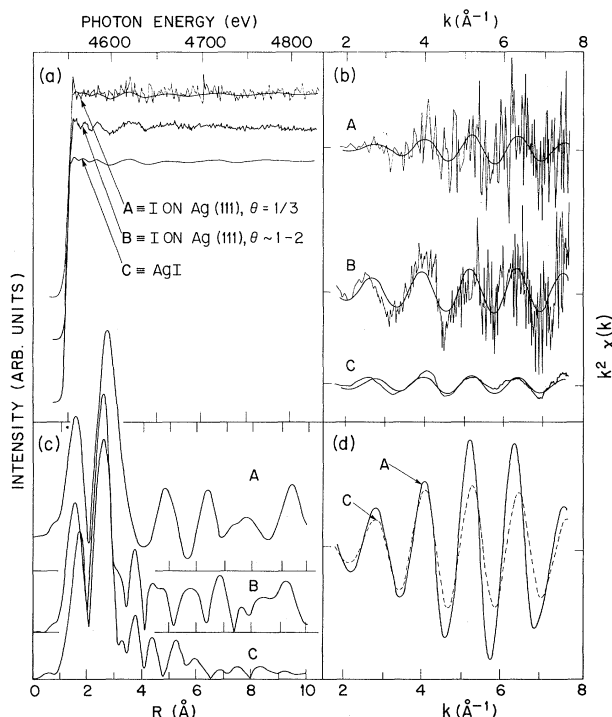


FIG. 1. (a) Raw data in energy space for three different I/Ag systems. Curves A and B are SEXAFS (Auger) spectra; curve C is an EXAFS (transmission) spectrum. Curve C is overlaid on curve A. (b) Raw data in momentum space after background subtraction and multiplication by  $k$  (Ref. 2). Smooth curves are retransformed and filtered data [see (d)]. (c) Fourier transforms in distance space of raw data from (b). The peaks at 2.6 Å have been arbitrarily set equal in height. (d) Normalized, retransformed data from (c) after filtering with a window from  $R = 1.6$  to  $3.8$  Å. Note differences in phase and amplitude.

processed exactly as above for the I-Ag(111) system. In Figs. 1(a)–1(c) we show the analogous results for the AgI analysis, and in Fig. 1(d) we have overlaid the normalized data of AgI (dashed line) with the corresponding data from I-Ag(111). Even at this stage it is apparent from the difference in phases that the I-Ag(111) bond length is larger than in AgI. It is straightforward to quantify this result from the data in Fig. 1(d) by extracting  $\varphi(k)$  for the I-Ag pair in AgI using a complex-Fourier-transform decomposition of phase and amplitude.<sup>7</sup> With the  $\varphi(k)$  from AgI and its I-Ag distance of  $R = 2.803 \text{ \AA}$ ,<sup>11</sup> we determine the I-Ag(111) distance to be  $2.87 \pm 0.03 \text{ \AA}$ . Analysis of a large sampling of computer-simulated data of variable signal/noise (significantly above and below that reported here) has confirmed the statistical accuracy of the quoted error limits. Experience with numerous other systems has shown that systematic errors in the data analysis procedure per se contribute  $\approx 0.01 \text{ \AA}$  error. By far the dominant source of uncertainty here arises from the present signal/noise [compare spectra *A* and *B* in Figs. 1(a)–1(c)]. To our knowledge this SEXAFS result is the most accurate determination of an adsorbate-substrate bond length.

The structural characterization of the I-Ag(111)

system is incomplete without knowledge of the adsorption site. The *single* distance in the SEXAFS data in Fig. 1(a)—and even that of the room-temperature AgI EXAFS data with superior signal/noise—indicates the predominance of nearest-neighbor scattering and thus in this system precludes site identification on the basis of next-nearest-neighbor distances.<sup>4</sup> It is possible, however, to determine the adsorption site from  $A(k)$ . For a single-distance system, and for strictly  $p-d$  dipole excitation,<sup>12,13</sup> this can be generally expressed by

$$A(k) \propto (N/kR^2) f(k, \pi) \exp(-2\sigma^2 k^2) e^{-2R/\lambda(k)},$$

$$N = \sum_i \frac{1}{3} + |\vec{\epsilon} \cdot \vec{r}_i|^2,$$

where  $f(k, \pi)$  is the backscattering amplitude,  $\exp(-2\sigma^2 k^2)$  is a Debye-Waller-like factor with rms deviation  $\sigma$ , and  $e^{-2R/\lambda(k)}$  is an inelastic loss term with mean electron escape depth  $\lambda$ .  $N$  is the effective coordination number determined from the projection of the polarization of the synchrotron beam  $\vec{\epsilon}$  onto the unit vector  $\vec{r}_i$  that connects the absorbing atom to the  $i$ th atom in the coordination sphere. Denoting the I-Ag(111) surface and AgI bulk systems by *S* and *B*, respectively, and assuming that  $\lambda(k)$  is comparable in both, we obtain

$$\ln[A_S(k)/A_B(k)] = \ln(N_S R_B^2 / N_B R_S^2) + 2k^2(\sigma_B^2 - \sigma_S^2) + 2(R_B - R_S)/\lambda(k).$$

The last term is negligible within our experimental uncertainty since  $2(R_B - R_S) \ll \lambda(k)$ . From the remaining linear plot in  $k^2$  and knowledge of  $R_S$  and  $R_B$  we can thus determine the effective coordination number of the adsorbed I atom, i.e., the adsorption site. [We can, of course, also determine  $(\sigma_B^2 - \sigma_S^2)$ , but because the AgI and I-Ag(111) data were taken at different temperatures we defer this question for a future study.] In Table I we have listed the values of  $N_S$  calculated for  $\vec{\epsilon}$  in the present experiment with adsorption sites of the symmetric onefold, twofold, and threefold coordination sites on the (111) surface. Also included is  $N_B$  for the tetrahedral coordination in polycrystalline AgI. Comparison of these calculated values with the experimentally determined  $N_S$  shows that *only* the threefold coordination site of adsorbed I lies within our experimental limits, consistent with the comparison approach in the earlier LEED study of Forstmann, Berndt, and Büttner.<sup>2</sup> In general, to determine the adsorption site more unambiguously—

in the absence of clearly observable second-nearest-neighbor distances—will require improved signal/noise and at least two measurements with the polarization directions parallel and perpendicular to the surface (lower-symmetry sites may require still an additional orthogonal measurement with  $\vec{\epsilon}$  in the surface plane).

In the first application of the SEXAFS technique, it is appropriate to point out its general strengths and limitations, as well as its future capabilities. As emphasized here, SEXAFS allows bond lengths of adsorbates to be determined

TABLE I. Values of  $N_S = \sum_i (\frac{1}{3} + |\vec{\epsilon} \cdot \vec{r}_i|^2)$  to determine adsorption site.

AgI (calc)	I-Ag(111) (calc)			I-Ag(111) (expt)
	1	2	3	
2.66	1.21	1.99	2.81	$3.2 \pm .8$

directly and accurately without reliance on multiple trial calculations. Temperature studies can also provide important information about Debye-Waller effects of surface atoms. In general, the adsorbates need not be ordered and the substrate need not be a single crystal. However, use of the polarization dependence of  $A(k)$  in single-crystal systems may be essential for distinguishing between adsorption sites when second-nearest-neighbor distances are not readily observable. The SEXAFS technique should be applicable to any adsorbate atom or molecule with  $Z \geq 6$  whose core Auger electrons are energetically resolvable from those of the substrate and other atoms in the molecule. For low- $Z$  adsorbates, however, the possible introduction with scanning photon energy of other Auger channels and/or primary photoemission from the substrate may require taking difference or partial-yield spectra. Future areas for development and improvement include more efficient and better-matched photon monochromators, thinner or removable Be windows, a more efficient energy analyzer, and more intense and brighter sources of synchrotron radiation. All of these areas, which are currently being developed, could enhance signal rates by as much as  $10^2$ – $10^4$  and allow data such as reported here to be taken in a matter of minutes or seconds.

In summary, the SEXAFS technique has been shown to be a valuable complementary surface probe. Coupled with Auger electron spectroscopy and LEED, it should make it possible to characterize with the same apparatus both the electronic structure of surfaces using photoemission and the short-range geometrical surface structure using SEXAFS.

The authors are indebted to G. P. Schwartz and H. H. Farrell for their assistance in experiments related to the present study. We are also grateful to P. A. Lee for stimulating discussions, B. M. Kincaid, J. E. Rowe, J. A. Appelbaum,

and D. R. Hamann for helpful comments and suggestions, M. M. Traum, N. V. Smith, and I. Lindau for their initial help and interest, and W. E. Spicer, G. P. Schwartz, and R. M. Madix for use of some key equipment in the preliminary stages of this work. The experiments were performed at Stanford Synchrotron Radiation Laboratory, which is partially supported by National Science Foundation Grant No. DMR 73-07692, in cooperation with the Stanford Linear Accelerator and U. S. Energy Research and Development Administration.

<sup>1</sup>See, for example, J. B. Pendry, *Low Energy Electron Diffraction* (Academic, New York, 1974); F. Jona, *Surface Sci.* **68**, 204 (1977), and references therein.

<sup>2</sup>F. Forstmann, W. Berndt, and P. Büttner, *Phys. Rev. Lett.* **30**, 17 (1973).

<sup>3</sup>P. H. Citrin, *Bull. Am. Phys. Soc.* **22**, 359 (1977); see also P. H. Citrin, P. Eisenberger, and R. C. Hewitt, *J. Vac. Sci. Technol.* **15**, 449 (1977).

<sup>4</sup>P. A. Lee, *Phys. Rev. B* **13**, 5261 (1976); U. Landman and D. L. Adams, *Proc. Nat. Acad. Sci. U. S. A.* **73**, 2550 (1976).

<sup>5</sup>J. Jaklevic, J. A. Kirby, M. P. Klein, A. S. Robertson, G. S. Brown, and P. Eisenberger, *Solid State Commun.* **23**, 679 (1977).

<sup>6</sup>P. H. Citrin and H. Farrell, to be published.

<sup>7</sup>B. M. Kincaid, P. H. Citrin, and P. Eisenberger, to be published.

<sup>8</sup>A separate study on very high signal/noise Ag EXAFS data confirms the reliability of this procedure so long as the same data lengths and filter widths are used in comparing two data sets; see text.

<sup>9</sup>P. H. Citrin, P. Eisenberger, and B. M. Kincaid, *Phys. Rev. Lett.* **36**, 1346 (1976).

<sup>10</sup>P. Eisenberger and G. S. Brown, to be published.

<sup>11</sup>R. W. G. Wyckoff, *Crystal Structures* (Interscience, New York, 1963), 2nd ed., p. 110.

<sup>12</sup>The probability for  $p \rightarrow s$  excitation is negligible in the present measurement; see S. M. Heald and E. A. Stern, *Phys. Rev. B* **16**, 5549 (1977); P. A. Lee, private communication.

<sup>13</sup>The authors gratefully acknowledge the assistance of E. A. Stern in pointing out the expression of  $N$  for  $p \rightarrow d$  excitation in Ref. 12.